Electrocatalysis (2017) 8:392–398
DOI 10.1007/s12678-017-0384-8

ORIGINAL RESEARCH

Nickel Nanoparticles for the Efficient Electrocatalytic Oxidation of Methanol in an Alkaline Medium

Meisong Guo[1] · **Yanan Yu**[1] · **Jingbo Hu**[1,2]

Published online: 20 May 2017

Abstract Nickel nanoparticles (NiNPs) are directly synthesized on an indium tin oxide electrode by ion implantation, which is a convenient, cost-effective, and environmentally friendly method. The morphology of the obtained electrode is characterized by scanning electron microscopy (SEM). The size of the nickel nanoparticles (NiNPs) is in the range of 50~125 nm based on SEM measurements. The general electrochemical behaviors of the modified electrode are characterized by electrochemical impedance spectroscopy (EIS). The electrocatalytic activity and stability are measured by cyclic voltammetry (CV) and chronoamperometry. The results confirm that the NiNPs/ITO electrode has substantial electrocatalytic activity towards the oxidation of methanol with good stability, indicating possible applications in direct methanol fuel cells.

Keywords Nickel nanoparticles · Electrocatalytic · Oxidation · Methanol

Introduction

In recent years, direct methanol fuel cells (DFMCs) have attracted a great deal of attention because of fossil fuel exhaustion and worsening environmental pollution [1, 2]. DMFCs have the advantages of high energy conversion efficiencies and power densities, eco-friendliness, and low operating temperature [3–5]. The most efficient catalysts for DMFCs are Pt-based catalyst [6–8], but their further commercial applications are restricted because of their high cost, slow kinetics, and low stability. To improve the performance of DMFCs, it is necessary to design and synthesize non-Pt materials for methanol oxidation with high activity and stability.

Nickel-based materials, especially nickel nanoparticles, have received increased attention because of their excellent electrocatalytic oxidation performance towards methanol and low-cost compared with Ag, Pt, and Pd [9–14]. Recently, many efforts have been devoted to the synthesis of nanosized nickel-based materials and their applications in DMFCs [15]. For instance, G. S. Ferdowsi et al. used the electroless method for the deposition of nickel nanoparticles on a graphite rod as a modified electrode to oxidize methanol [10]. R.H. Tammam et al. fabricated binary catalysts composed of NiOx and MnOx nanoparticles on a modified glassy carbon electrode (GC) with controlled loading and order of the deposition for the electrocatalytic oxidation of methanol [16]. Recently, Joan Vilana et al. electrochemically synthesized CoNi nanorods of similar compositions (Co_7Ni_3 and Co_6Ni_4) but different crystalline phases (main hcp and hcp + fcc) for the electrooxidation of methanol [17].

The processes to prepare these electrodes are complicated and time consuming. In addition, to prepare electrode materials that exhibit high electrocatalytic performance, most of the catalysts must be effectively immobilized on the electrode surface. However, the methods of fabricating electrodes in most previous reports are traditional preparation processes which use polymer binders or carbon black as the conductive agent. However, the polymer binder will increase interfacial resistance, block active sites and inhibit diffusion, leading to decreased catalytic performance [18, 19]. These problems can be solved by the ion implantation method. The versatility of the implantation technique arises from the fact that almost all

✉ Jingbo Hu
hujingbo@bnu.edu.cn

[1] College of Chemistry, Beijing Normal University, Beijing 100875, People's Republic of China

[2] Key Laboratory of Beam Technology and Material Modification of Ministry of Education, Beijing Normal University, Beijing 100875, People's Republic of China

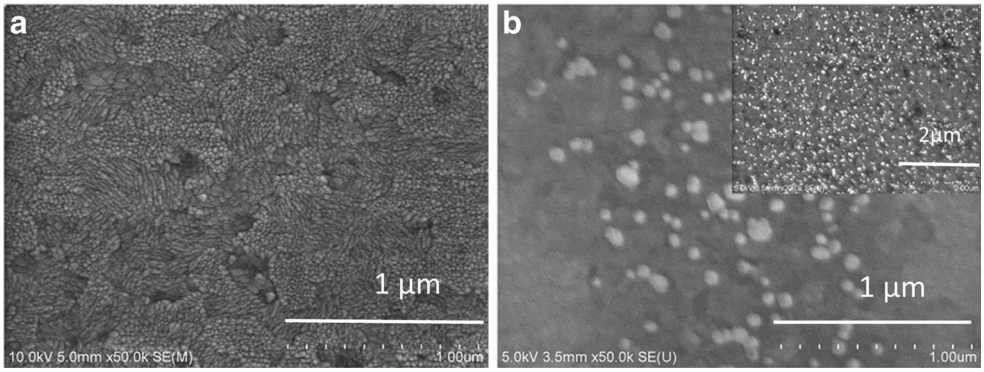

Fig. 1 SEM of the bare ITO (**a**) and the NiNPs/ITO electrode (**b**)

elements in the periodic table can be implanted into virtually any selected host material. In addition, the process is facile, inexpensive and eco-friendly without using any other chemicals. Compared with chemical vapor deposition [20], sol–gel methods [21], carbon nanotube compositing processes, and other modification methods [22, 23], ion implantation is more convenient for the formation of metal nanoparticles on many kinds of substrates [24, 25]. Electrodes prepared by ion implantation without a binder or conducting agent are able to create nanocomposite materials with good electroactivity. Indium tin oxide (ITO) coated on glass was used as an electrode substrate and working electrode. It has the advantages of excellent optical transparency, high electrical conductivity, a wide electrochemical working window, low capacitive current, and stable electrochemical and physical properties [26–28].

In the present study, we prepared nickel nanoparticle-modified ITO electrodes (NiNPs/ITO) by the ion implantation method. The as-prepared electrodes were characterized by SEM to investigate whether the nickel nanoparticles were successfully implanted on the ITO surface. The electrocatalytic activity and stability towards electrooxidation of methanol was studied in an alkaline medium by cyclic voltammetry and chronoamperometry. The results indicate that the nickel nanoparticles significantly enhance the electrical conductivity of the bare ITO electrode, and the NiNPs/ITO electrode shows remarkable catalytic activity and good stability for the electrooxidation of methanol.

Experimental

Reagents

ITO glass was purchased from Beijing Tsinghua Engineering Research Center of Liquid Crystal Technology. The chemicals were all of analytical grade and used as purchased without any further purification. All measurements were performed at room temperature. All solutions were prepared with triply distilled water.

Preparation of the NiNPs/ITO Electrode

Ion implantation was carried out using a Beijing Normal University (BNU) metal vapor vacuum arc (MEVVA) implanter. Before ion implantation, the ITO surface was cleaned ultrasonically in triply distilled water, then ethanol, and then again with triply distilled water for 5 min. Then, the ITO was dried by nitrogen gas at room temperature. Nickel ions with 10 keV at the fluence of 10×10^{17} ions cm^{-2} were implanted onto the pretreated ITO surface, forming the NiNPs/ITO electrode. Bare or modified ITO (3 mm × 10 mm) were washed with distilled water and absolute ethanol several times before being used.

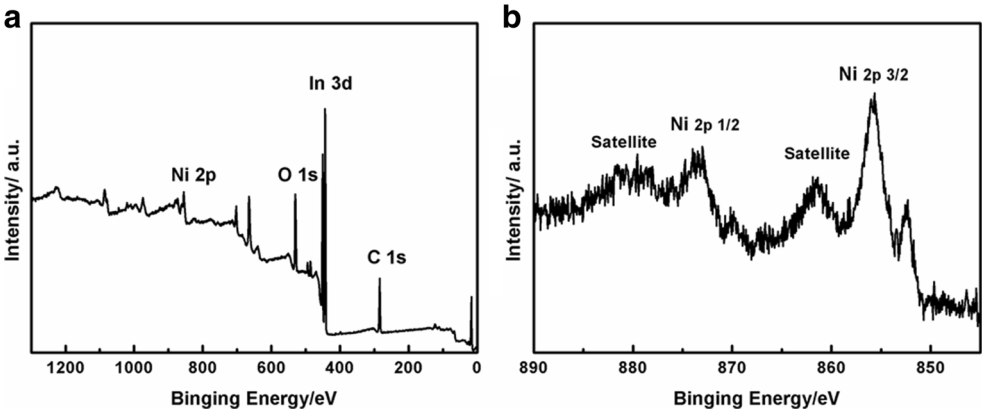

Fig. 2 XPS spectra of NiNPs/ITO

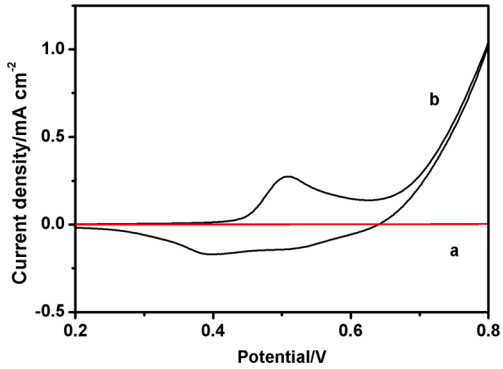

Fig. 3 CV of the bare ITO (*a*) and the NiNPs/ITO electrode (*b*) in 1 M NaOH at a scan rate of 50 mV s^{-1}

Apparatus

The structure and morphology of the electrode were characterized by scanning electron microscope (SEM) (Hitachi X650, Japan). The electrochemical measurements were conducted in a three-electrode single-cell system in the electrolyte (1 M NaOH) containing methanol at various concentrations. Bare or modified ITO (A = 30 mm^2), Ag/AgCl and platinum wire electrodes were used as the working, reference and counter electrodes, respectively. The NiNPs/ITO electrode was activated by cycling the potential from −0.2 to 0.8 V in 0.1 NaOH about 20 cycles at the scan rate of 50 mV s^{-1} before electrochemical experiments.

Results and Discussion

Characterization of NiNPs/ITO Electrode

SEM Images of NiNPs/ITO Electrode

We have changed the Ni content by changing the implantation fluences in our previous researches [25, 29, 30]. The particle size was almost the same when we changed the fluences from 5.0×10^{16} ions cm^{-2} to 20.0×10^{16} ions cm^{-2}. By comparing these fluences, we found that the fluence at 10.0×10^{16} ions cm^{-2} is optimal, so we choose this fluence for the current study. The surface morphologies of the bare ITO and the NiNPs/ITO were characterized by SEM. As shown in Fig. 1a, there are some gullies and spherical grains on the bare ITO electrode surface. After the ion implantation of nickel on the bare ITO electrode, the surface becomes smooth and the spherical features of the bare ITO disappear because of the sputtering effect of the implantation of nickel ions. We can easily find the nickel nanoparticles dispersed uniformly on the surface of ITO using the high magnification SEM image (Fig. 1b). The size of nickel nanoparticles ranges from 50 to 125 nm. The results above show that the nickel nanoparticles have been successfully synthesized on the surface of the ITO electrode.

XPS Spectra of NiNPs/ITO Electrode

In order to investigate the surface composition of NiNPs/ITO, XPS was used to determine the chemical state of the product. It demonstrates that the signals of In 3d, O 1 s, C 1 s, and Ni 2p are detected based on the full scan spectra (Fig. 2a). The signals of In 3d, O 1 s, and C 1 s are indexed to ITO substrate. The Ni 2p spectrum is shown in Fig. 2b, and two major peaks at 873.02 and 855.78 eV are indexed to Ni^{2+}. The XPS spectra demonstrate the existence of Ni nanoparticles on the surface of ITO substrate.

Electrochemical Behaviors of the NiNPs/ITO Electrode with CV

The bare ITO and the NiNPs/ITO electrodes were first characterized using cyclic voltammetry (CV), as shown in Fig. 3. It was clear that no obvious oxidation/reduction peaks were observed on the bare ITO. The NiNPs/ITO electrode was activated in 0.1 M NaOH before electrocatalytic texts for

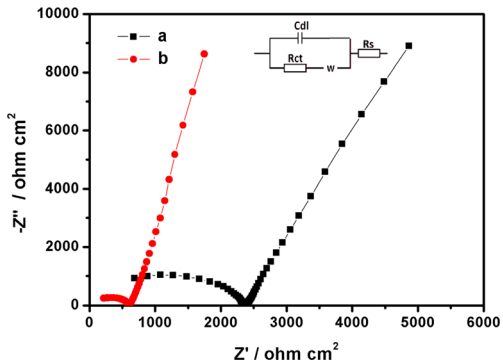

Fig. 4 Nyquist impedance plots of NiNPs/ITO electrode with (*a*) and without (*b*) 1 M methanol in the presence of 0.1 M NaOH. Frequency range 100 KHz to 1 Hz. The inset shows the equivalent circuit used for fitting of EIS date

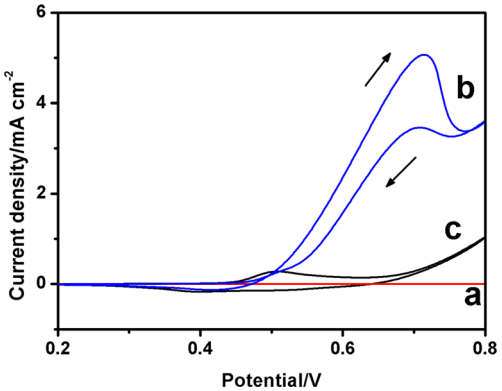

Fig. 5 CV of the bare ITO (*a*) and the NiNPs/ITO (*b*) in the presence of 0.5 M methanol and the NiNPs/ITO without methanol (*c*) in 1 M NaOH. Scan rate 50 mV s^{-1}

Table 1 Comparison of NiNPs/ITO with other modified electrodes

Composites	Electrolyte	T (°C)	Concentration (M)	Peak potential	Peak current density (mA cm^{-2})	Scan rate mV/s	Reference
NiNPs/ITO	0.1 M NaOH	Room temperature	0.5	710 vs. Ag/AgCl	5.47	50	This work
CPE/poly-Ni(II)-quercetin	0.1 M NaOH	Room temperature	0.1	580 vs. SCE	0.75	20	[39]
GC/MnOx/NiOx	0.5 M NaOH	Not mentioned	0.5	530 vs.SCE	16.67	20	[33]
NiNP-GE	0.5 M NaOH	Not mentioned	0.5	800 vs.SCE	7	100	[10]
GC/poly-Ni(II)TCPP	0.1 M NaOH	Room temperature	0.1	680 vs. SCE	2.23	20	[40]
MWCNTPE/poly-Ni(II)-quercetin	0.1 M NaOH	Room temperature	0.1	580 vs. SCE	6.47	20	[39]

methanol oxidation to create the NiOOH species with highly electrocatalytic activity. After activation, we detected two peaks in the voltammogram. One is in the anodic direction at 0.509 V due to the formation of NiOOH, and the other in the cathodic direction at 0.398 V originating from the reduction of NiOOH, as per the following reaction:

$$Ni + 2OH^- \rightarrow Ni(OH)_2 + 2e^- \quad (1)$$

$$Ni(OH)_2 + OH^- \rightleftarrows NiOOH + H_2O + e^- \quad (2)$$

This result suggests the successful formation of NiNPs/ITO. By comparing the electrochemical behaviors of the NiNPs/ITO and bare ITO electrodes with CV, we believe that the modified electrode has better electrochemical activity than the bare ITO electrode.

Electrochemical Behaviors of the NiNPs/ITO Electrode with EIS

In order to investigate the effect of doping nickel ions on bare ITO electrode, EIS measurement was used to further study the internal resistance, electron-transfer kinetics, and ion diffusion process of the obtained electrodes. Figure 4 shows the Nyquist impedance plots of NiNPs/ITO electrode with (a) and without (b) 1 M methanol in the presence of 0.1 M NaOH measured at 0.55 V (vs. Ag/AgCl) in the frequency range of 100 kHz to 1 Hz.

As shown in Fig. 4, Nyquist plots of NiNPs/ITO electrode exhibit a semicircular shape in the high frequencies, which related to the combination of the Rct of transformation between NiOOH and $Ni(OH)_2$ on the surface [31]. The Rct of NiNPs/ITO electrode in 1 M methanol is 600 Ω cm^{-2}, which is much smaller than without methanol (2400 Ω cm^{-2}). It suggests that the charge-transfer resistance is lower after adding methanol to the electrolyte. What is more, the Rct of NiNPs/ITO electrode is smaller than other similar electrodes, such as NiO/foam Ni electrode [32], GC/NiOx electrode [33], and G/NiCuCo electrode [34], which demonstrates that NiNPs/ITO electrode owns good electrocatalytic activity. At low frequencies, the phase angle is related to the Warburg resistance, which is account for the diffusion of ions to the interface between electrode and electrolyte. In this work, the Nyquist plot of NiNPs/ITO electrode with 1 M methanol shows more close to vertical line at low frequencies of the complex impedance, indicating the existence of constant phase element (CPE) and the diffusion of methanol into the porous NiNPs/NF electrode is a limiting process [35].

The Electrocatalytic Oxidation of Methanol

Figure 5 shows the CV of the bare ITO (a), the NiNPs/ITO (b) in the presence of 0.5 M methanol, and the NiNPs/ITO without methanol (c) in 1 M NaOH. We did not find any peaks on the bare ITO in the presence of 0.5 M methanol (curve a). From curve b, two oxidation peaks appeared after adding

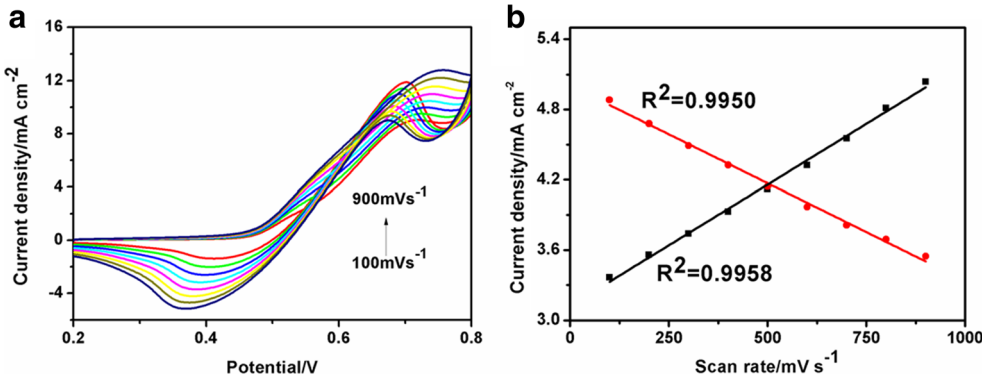

Fig. 6 **a** CV of the NiNPs/ITO in the presence of 0.5 M methanol in 1 M NaOH at various scan rates from 100 to 900 mV s^{-1}. **b** The linear relationship of the oxidation peak currents with various scan rates

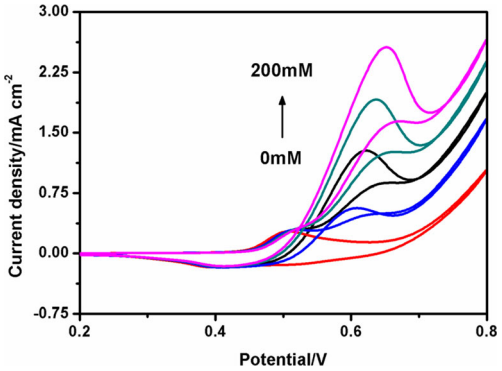

Fig. 7 CV of the NiNPs/ITO electrode with different concentrations of methanol in 1 M NaOH solution, scan rate 50 mV s^{-1}

methanol. The redox transition of nickel species present in the film is the following:

$$\text{Ni (II)} \rightleftarrows \text{Ni (III)} + \text{e-} \quad (3)$$

Several mechanisms have been reported regarding the electrooxidation of methanol on nickel-based materials in alkaline solution. Fleischmann et al. proposed a mechanism of methanol oxidation and suggested that the NiOOH acts as an electrocatalyst [36, 37]. Taraszewska et al. considered that methanol oxidation occurs after complete conversion of $Ni(OH)_2$ to NiOOH due to an anodic potential sweep [38]. On the basis of the above literature, we consider the mechanism for the mediated electrooxidation of methanol on the NiNPs/ITO electrode to be the following series of reactions:

$$Ni^{3+} + \text{methanol} \rightarrow Ni^{3+} + \text{intermediate} \quad (4)$$

$$Ni^{3+} + \text{intermediate} \rightarrow Ni^{2+} + \text{products} \quad (5)$$

Table 1 shows the comparison of peak potentials and peak current densities of the NiNPs/ITO towards methanol electrooxidation with some of the modified electrodes, such as CPE/poly-Ni(II)-quercetin, NiNP-GE, and GC/poly-Ni(II)TCPP. Although the quantity of nickel ions implanted onto the pretreated ITO surface was very low, the peak current density of NiNPs/ITO electrode still comparable with other modified electrodes and shows good catalytic activity for methanol oxidation. In addition, the preparation of the NiNPs/ITO electrode is much easier than other electrodes. Thus, the NiNPs/ITO electrode has the unique advantages of easy preparation; economic and environmentally friendly will be a promising electrocatalyst for methanol oxidation.

Fig. 6a shows the CV of the NiNPs/ITO electrode in the presence of 500 mM methanol in 1 M NaOH at scan rate from 100 to 900 mV s^{-1}. The results demonstrate that the two anodic peaks are linearly proportional to the scan rate (Fig. 6b) with a correlation coefficient of 0.9950 and 0.9958. This suggests that the methanol electrooxidation is a surface-controlled process. According to Fig. 6, we find that with the increasing scan rates, the oxidation peak current of Ni^{2+} in the positive sweep is increasing and the oxidation peak in the negative sweep is decreasing. This can be attributed to the fact that when the scan rates increase, it becomes too fast for the following chemical reaction (Eqs. 4 and 5), which can regenerate Ni (II). This result is highly consistent with the above analysis. In addition, the anodic peak potential in the positive/negative sweep displays positive/negative shifts due to the polarization of the electrodes.

The effect of the methanol concentration was also investigated. Figure 7 shows a cyclic voltammogram of the NiNPs/ITO electrode in a 1 M NaOH solution in the presence of various concentrations of methanol ranging from 50 to 200 mM and at scan rate of 50 mV s^{-1}. As the figure shows, the two oxidation peak currents increase with increasing methanol concentrations because of the higher methanol concentration is present, the more NiOOH reduces to $Ni(OH)_2$. With the methanol concentration increasing, the NiOOH consumption is increasing and the residual amount of NiOOH on the catalysis surface is decreasing, which lead to the lower reduction current density [5]. The electrocatalytic current of methanol shows good linearity with methanol concentrations ranging from 50 to 200 mM. In addition, the peak potential of two oxidation peaks moves in the positive direction with the concentration increasing, which indicate that the methanol oxidation reaction rate become slower.

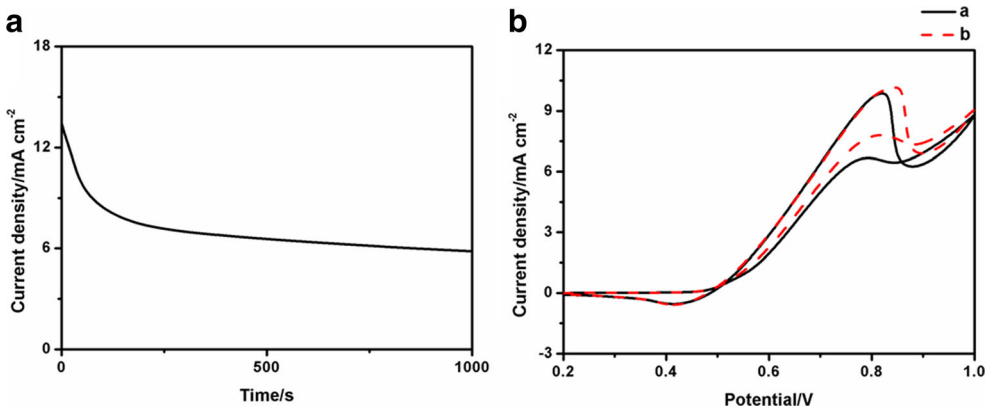

Fig. 8 **a** Chronoamperometric responses of the NiNPs/ITO in 1 M NaOH towards 1 M methanol. **b** The recovery ability of the NiNPs/ITO electrode after 1000 continuous cycles: *curve a*, the first cycle, and *curve b*, the 1001st cycle in freshly prepared solution (1 M methanol +1 M NaOH)

The stability of the NiNPs/ITO electrode was studied by chronoamperometry and cyclic voltammetry. Figure 8a shows the chronoamperometric curves of the NiNPs/ITO electrode in a solution of 1 M NaOH for 1 M methanol oxidation at a constant potential of 0.8 V versus Ag/AgCl for 1000 consecutive seconds. After a rapid initial decay, the current density reached a steady state, which indicates a high stability. This result suggests that the NiNPs/ITO electrode has good electrochemical stability during the short duration for the oxidation of methanol. The proposed modified electrode was stored in air at ambient conditions, and its sensitivity was checked every month by cyclic voltammetry. The response was 93% of its initial value after 6 months, which shows the long-term stability of this electrode for the oxidation of methanol. The cycling performance of the NiNPs/ITO electrode towards the oxidation of methanol is shown in Fig. 8b. The peak current at 0.79 and 0.82 V of methanol oxidation from the forward CV sweep increased slightly as the cycle number increased. After scanning 1000 CV cycles, a CV measurement was performed on the catalyst again in freshly prepared 1 M methanol and 1 M NaOH aqueous solution. The two oxidation peak current responses were 116.8 and 102.8% compared to the response in the first cycle. The high stability of NiNPs/ITO further implies that ion implanted NiNPs will be a good alternative catalyst in fuel cells.

Conclusions

Nickel nanoparticles were successfully synthesized on the surface of ITO by ion implantation, which is a facile and environmentally friendly method. The NiNPs/ITO electrode exhibits good catalytic activity and electrochemical stability for the electrooxidation of methanol in an alkaline medium. These excellent electrochemical properties can be attributed to the direct implantation of Ni nanoparticles without the use of any polymer binders, which reduce the interface resistance and improve the electrical conductivity. In summary, NiNPs/ITO electrodes with these novel functions are excellent candidates for active, stable, and low-cost direct methanol fuel cells and could be used in large-scale industrial applications in the future.

Acknowledgments This research was supported by the Fundamental Research Funds for the Central Universities and the National Natural Science Foundation of China (Grant No. 21590801).

References

1. Q. Luo, M.Y. Peng, X.P. Sun, A.M. Asiri, Catal. Sci. Technol. **6**, 1157 (2016)
2. W. Wang, Q.X. Chu, Y.N. Zhang, W. Zhu, X.F. Wang, X.Y. Liu, New J. Chem. **39**, 6491 (2015)
3. L. Qian, W. Chen, R.F. Huang, D. Xiao, RSC Adv. **5**, 4092 (2015)
4. Z. Wang, Y. Du, F. Zhang, Z. Zheng, Y. Zhang, C. Wang, J. Solid State Electrochem. **17**, 99 (2012)
5. L.S. Yuan, Y.X. Zheng, M.L. Jia, S.J. Zhang, X.L. Wang, P. Cheng, Electrochim. Acta **154**, 54 (2015)
6. W.E. Mustain, H. Kim, V. Narayanan, T. Osborn, P.A. Kohl, Plant J. **83**, 300 (2015)
7. Z. Bo, D. Hu, J. Kong, J. Yan, K. Cen, J. Power Sources **273**, 530 (2015)
8. Y. Li, L. Tang, J. Li, Electrochem. Commun. **11**, 846 (2009)
9. A.N. Golikand, M. Asgari, M.G. Maragheh, S. Shahrokhian, J. Electroanal. Chem. **588**, 155 (2006)
10. G.S. Ferdowsi, S.A. Seyedsadjadi, A. Ghaffarinejad, J. Nanostruct. Chem. **5**, 1 (2014)
11. X. Tarrús, M. Montiel, E. Vallés, E. Gómez, Int. J. Hydrog. Energy **39**, 6705 (2014)
12. P.R. Jothi, S. Kannan, G. Velayutham, J. Power Sources **277**, 350 (2015)
13. C. Xun, G. Wenlong, Z. Ming, Y. Yang, L. Yanhong, X. Peng, Z. Yunhuai, Z. Xiaoxing, ACS Appl. Mater. Interfaces **7**, 493 (2015)
14. C.-W. Roh, J.-Y. Seo, C.-H. Chung, Sci. Adv. Mater. **8**, 34 (2016)
15. K. Kakaei, K. Marzang, J. Colloid Interface Sci. **462**, 148 (2016)
16. R.H. Tammam, A.M. Fekry, M.M. Saleh, Int. J. Hydrog. Energy **40**, 275 (2015)
17. J. Vilana, D. Escalera-López, E. Gómez, E. Vallés, J. Alloy. Compd. **646**, 669 (2015)
18. Y. Luo, J. Jiang, W. Zhou, H. Yang, J. Luo, X. Qi, H. Zhang, D.Y.W. Yu, C.M. Li, T. Yu, J. Mater. Chem. **22**, 8634 (2012)
19. J.B. Wu, Z.G. Li, X.H. Huang, Y. Lin, J. Power Sources **224**, 1 (2013)
20. Y. Mei, J. Chen, J. Liu, S. Li, Y. Ma, J. Zhang, J. An, Electrochim. Acta **151**, 99 (2015)
21. M.J. Alam, D.C. Cameron, Thin Solid Films **76**, 420 (2002)
22. V.K. Gupta, A.K. Jain, S. Agarwal, G. Maheshwari, Talanta **71**, 1964 (2007)
23. R.N. Goyal, V.K. Gupta, S. Chatterjee, Klin. Med. **149**, 252 (2010)
24. W. Su, Y.Y. Fu, T. Wang, Y.N. Yu, J.B. Hu, RSC Adv. **5**, 79178 (2015)
25. Y. Yu, W. Su, M. Yuan, Y. Fu, J. Hu, J. Power Sources **286**, 130 (2015)
26. Y. Niidome, H. Hisanabe, T. Kawasawa, S. Yamada, Thin Solid Films **513**, 60 (2006)
27. Y. Song, Y. Ma, Y. Wang, J. Di, Y. Tu, Electrochim. Acta **55**, 4909 (2010)
28. Y. Fu, F. Liang, H. Tian, J. Hu, Electrochim. Acta **120**, 314 (2014)
29. H. Tian, M. Jia, M. Zhang, J. Hu, Electrochim. Acta **96**, 285 (2013)
30. H. Tian, F. Liang, J. Jiao, J. Hu, J. Electrochem. Soc. **160**, B125 (2013)
31. W. Shi, H. Gao, J. Yu, M. Jia, T. Dai, Y. Zhao, J. Xu, G. Li, Electrochim. Acta **220**, 486 (2016)

32. L. Wang, Y. Xie, C. Wei, X. Lu, X. Li, Y. Song, Electrochim. Acta **174**, 846 (2015)
33. R.H. Tammam, A.M. Fekry, M.M. Saleh, Int. J. Hydrog. Energy **40**, 275 (2014)
34. T. Rostami, M. Jafarian, S. Miandari, M. Gmahjani, F. Gobal, D.O. Chemistry, Chin. J. Catal. **36**, 1867 (2015)
35. J. Bisquert, G. Garcia-Belmonte, P. Bueno, E. Longo, L.O.S. Bulhões, J. Electroanal. Chem. **452**, 229 (1998)
36. M. Fleischmann, K. Korinek, D. Pletcher, J. Electroanal, Chem **31**, 39 (1971)
37. M. Fleischmann, K. Korinek, D. Pletcher, J. Chem. Soc. Perkin Trans. **2**, 1396 (1972)
38. J. Taraszewska, G. Rosłonek, J. Electroanal. Chem. **364**, 209 (1994)
39. L. Zheng, J.F. Song, J. Solid State Electrochem. **14**, 43 (2010)
40. M. Jafarian, M.A. Haghighatbin, F. Gobal, M.G. Mahjani, S. Rayati, J. Electroanal. Chem. **663**, 14 (2011)